Supporting Information

Rapid Discovery of Yttrium-MOFs via Combined High-Throughput Synthesis, Automated PXRD, Optical Calorimetry Screening and Three-dimensional Electron Diffraction

*Lasse Wegner,[a] Zheting Chu[c], Tobias A. Engesser[a], Xiaodong Zou[c] and Norbert Stock[ab]**

[a] Institute for Inorganic Chemistry, Kiel University, Max-Eyth Straße 2, 24116 Kiel, Germany.

[b] Kiel Nano, Surface and Interface Science KiNSIS, Kiel University, Christian-Albrechts-Platz 4, 24118 Kiel, Germany.

[c] Department of Chemistry, Stockholm University, Svante Arrhenius Väg 16 C, 106 91 Stockholm, Sweden.

Table of contents

Materials and methods

The chemicals used in this study were bought from commercial suppliers and used without further purification.

Powder X-ray diffraction data at room temperature was collected on a Stoe Stadi P diffractometer in transmission geometry with Cu $K_{\alpha 1}$ radiation equipped with a Mythen 1K detector. For the HT-PXRD screening a xy-sample holder for the automated measurement of up to 48 samples was used. Water sorption isotherms at 298 K and N_2 sorption isotherms at 77 K were collected on a BELSORP-max apparatus. CO_2 sorption isotherms were collected on a BELSORP MiniX at 298 K. For all volumetric sorption experiments, the samples were activated under reduced pressure at 200 °C before starting the measurements. Elemental analysis was performed with a vario MICRO cube elemental analyzer from Elementar Analysensysteme GmbH. IR spectra were recorded at room temperature on a Bruker Vertex 70 FT-IR spectrometer using a broadband spectral range extension VERTEX FM for full mid and far IR in the range of 6000 - 80 cm^{-1}. For the temperature resolved infrared spectroscopy the spectra were measured in diffuse reflection by using the Praying Mantis™ Diffuse Reflection Accessory of Harrick Scientific Products in the Bruker Vertex 70 FT-IR spectrometer. The sample was combined with twice the sample mass of potassium bromide and ground in a mortar before the measurement. Thermogravimetric (TG) measurements were performed on a Linseis STA 1600 analyzer with a heating rate of 8 K/min in air. Scanning electron microscopy was carried out using a SU8700 scanning electron microscope from Hitachi with an acceleration voltage of 3 kV. Screening for CO_2 adsorption was measured with a INFRAsorp optical calorimeter from Fraunhofer IWS equipped with an automatic sample changer for 12 samples. The samples were placed in the device at ambient conditions and measured for 10 cycles each. Adsorption was performed by flowing a CO_2 stream of 337.5 sccm through the sample for 90 s while desorption was accomplished by purging with dry N_2 with 250 sccm for 120 s. The variable-temperature PXRD (VT-PXRD) measurements were performed by using a Bruker D8 Discover powder diffractometer (Cu Kα1,2 radiation) equipped with a XRK 900 chamber. The analyzed sample was heated in defined temperature steps from 50 °C to 400 °C, and a series of PXRD patterns were recorded. For 3D ED data collection, the sample was gently crushed, dispersed in pure water, and sonicated for 20 seconds before depositing onto a lacey carbon film supported Cu TEM grid. 3D ED data was collected using the continuous rotation electron diffraction (cRED) technique.[1] Measurements were performed at 100 K, 298 K, and 523 K on a JEOL JEM-2100 transmission electron microscope operated at 200 kV, equipped with a highspeed hybrid Timepix camera (Amsterdam Scientific Instruments) and controlled by Instamatic (v1.0.0) software.[2]

Synthesis

The initial HT-screening consisted of 24 separate reactions in 2 mL steel multiclaves with Teflon inserts. Two commercially available N-heteroaromatic linker molecules were selected with no MOF structures reported in the CCDC database, 2,4-quinoline dicarboxylic acid and 2,5-indole dicarboxylic. They were reacted with 12 different metal salts respectively containing the elements zinc, copper, manganese, chromium, yttrium, magnesium, calcium, bismuth, lead, cobalt, nickel and tungsten to screen cations with different oxidation states and coordination numbers. To increase the reactivity of the linkers they were employed as aqueous solution of their disodium salts with a concentration of 0.5 mol/L. The linkers and metals were reacted in a 1:1 ratio at 120 °C for 256 h with heating and cooling steps of 72 h. The exact synthesis conditions can be found in Table S2. To reduce the synthesis time, the synthesis leading to **CAU-73** was repeated in a microwave oven at the 5 mL scale, decreasing the synthesis time from 400 h down to 6 h.

For the synthesis of **CAU-73**, 61.5 mg (0.3 mmol) of H_2IDC were mixed with 115 mg (0.3 mmol) of $Y(NO_3)_3 \cdot 6\,H_2O$, 4200 µL water and 300 µL of an aqueous solution of NaOH (c = 1 mol/L) in a 10 mL glass tube equipped with a magnetic stir bar. The reactor was closed with a Teflon septum and an aluminum cap and the reaction was carried out in a Biotage Initiator+ microwave reaction system at 150 °C for 6 h with continuous stirring. The product was isolated via filtration and subsequent washing with water and acetone and dried over night at ambient conditions. Yield: 48.8 %, based on the amount of 2,5-indole dicarboxylic acid.

Structure determination

The crystal structures of **CAU-73** compounds under 100 K, 298 K, and 523 K were determined by 3D ED. A batch of 3D ED data was processed through the AutoLEI[3] data processing pipeline, which utilizes XDS[4] as the data processing engine. The structures were solved *ab initio* using SHELXT[5] and all non-hydrogen atoms were found. The structures were refined anisotropically using SHELXL[6] in Olex2[7].

CCDC Database search

Comparing the deposited structures in the MOF-subset of the Cambridge Crystallographic Data Centre (CCDC) database that contain derivatives of benzene dicarboxylate to those that contain derivatives of pyridine dicarboxylate acid returns 22 554 and 2 672 hits respectively. With increasing complexity of the aromatic core, the difference between reported structures containing nitrogen heteroatoms and those without is even higher. Searches for structures based on naphthalene dicarboxylate yield 1 518 hits in the MOF-subset of the CCDC-database while the search for MOFs with a quinoline core results in 34 hits and those for indole dicarboxylates only 2 (Figure S1, as of 23.09.2025).

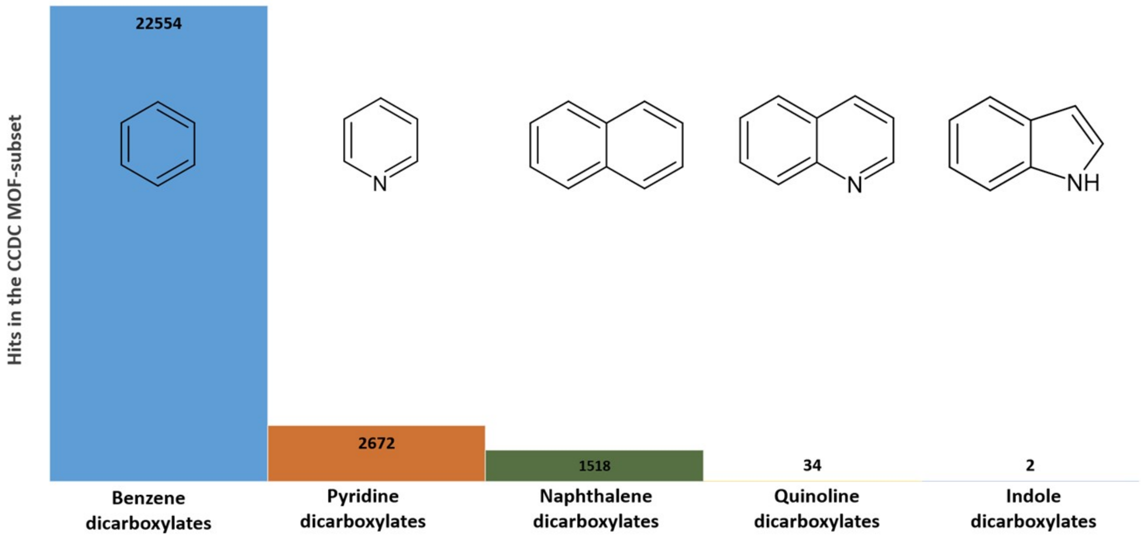

Figure S1: Hits in the CCDC database MOF-subset for structures containing dicarboxylates with different aromatic cores including all possible substitution combinations. Results containing more than two carboxylate groups were not counted.

Determination of the composition

To confirm the bulk composition of **CAU-73**, thermogravimetric and elemental analyses were conducted. The results are in good agreement with the sum formulas obtained from their respective crystal structures.

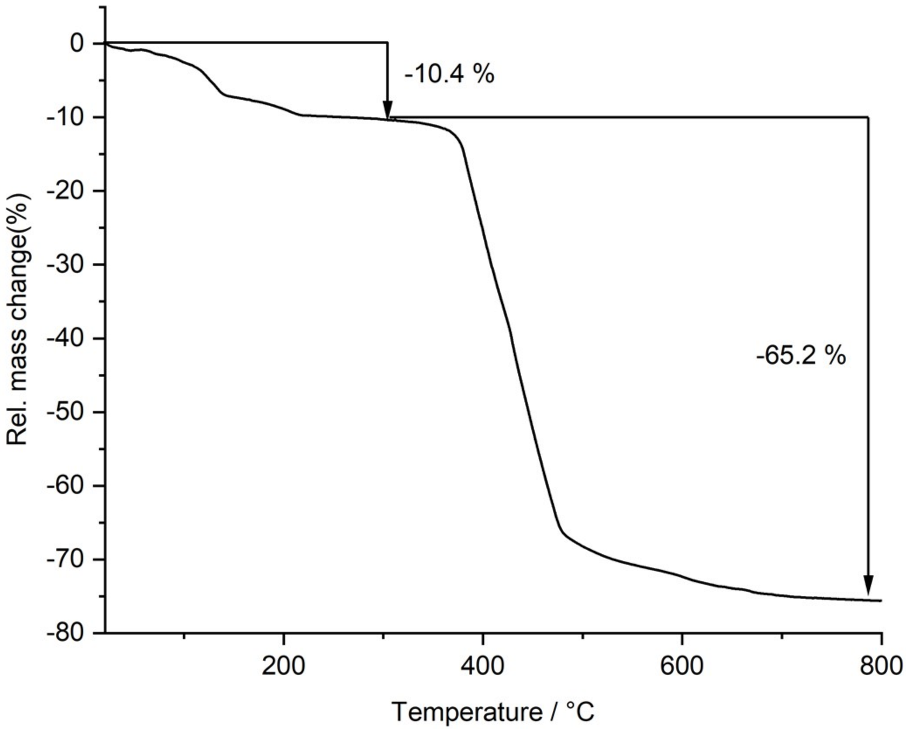

Figure S2: TG curve of **CAU-73**.

Table S1: Comparison of the experimental results from TG and elemental analysis with the postulated composition of **CAU-73**.

	C / %	H / %	N / %	1. TG step / %	2. TG step / %
Experimental	41.8	2.7	4.9	10.4	65.2
$[Y_2(IDC)_3(H_2O)_2] \cdot 2.2\ H_2O$	41.8	2.7	4.9	8.8	65.1

The sum formula obtained from CHNS and TG data differs in the water content compared to the one obtained from cryo-3D ED by 1.7 H_2O molecules, which can be explained by the different pressures and temperatures at which the measurements were conducted.

HT-Screening

For the initial HT-screening 2,4-quinoline dicarboxylic acid and 2,5-indole dicarboxylic were reacted with 12 different metal salts respectively. The linkers were employed as aqueous solution of their disodium salts with a concentration of 0.5 mol/L and combined with the metal salts in a 1:1 ratio in 2 mL steel multiclaves with Teflon inlets and a filling level of 960 µL.

The reaction was carried out in a convection oven at 120 °C for 256 h with a heating and cooling step of 72 h each. The precise amount of all reactants used are given in table S2. The products were isolated via vacuum filtration and washed with water and acetone and left to dry in air.

Table S2: List of all the reactants used in the HT-screening.

	Metal salt		2,4-Na_2QDC 0.5 mol/L		2,5-Na_2IDC 0.5 mol/L		H_2O
	µmol	mg	µmol	µL	mmol	µL	µL
$ZnCl_2$	60	8.2	60	120			840
$CuCl_2 \cdot 2\,H_2O$	60	10.2	60	120			840
$MnCl_2 \cdot 4\,H_2O$	60	11.9	60	120			840
$CrCl_3 \cdot 6\,H_2O$	60	16.0	60	120			840
$Y(NO_3)_3 \cdot 6\,H_2O$	60	23.0	60	120			840
$Mg(NO_3)_2 \cdot 6\,H_2O$	60	15.4	60	120			840
$CaCl_2 \cdot 2\,H_2O$	60	8.8	60	120			840
$Bi(NO_3)_3 \cdot 5\,H_2O$	60	29.1	60	120			840
$PbCl_2$	60	16.7	60	120			840
$CoCl_2 \cdot 6\,H_2O$	60	14.3	60	120			840
$NiCl_2 \cdot 6\,H_2O$	60	14.3	60	120			840
$Na_2O_4W \cdot 2\,H_2O$	60	19.8	60	120			840
$ZnCl_2$	60	8.2			60	120	840
$CuCl_2 \cdot 2\,H_2O$	60	10.2			60	120	840
$MnCl_2 \cdot 4\,H_2O$	60	11.9			60	120	840
$CrCl_3 \cdot 6\,H_2O$	60	16.0			60	120	840
$Y(NO_3)_3 \cdot 6\,H_2O$	60	23.0			60	120	840
$Mg(NO_3)_2 \cdot 6\,H_2O$	60	15.4			60	120	840
$CaCl_2 \cdot 2\,H_2O$	60	8.8			60	120	840
$Bi(NO_3)_3 \cdot 5\,H_2O$	60	29.1			60	120	840
$PbCl_2$	60	16.7			60	120	840
$CoCl_2 \cdot 6\,H_2O$	60	14.3			60	120	840
$NiCl_2 \cdot 6\,H_2O$	60	14.3			60	120	840
$Na_2O_4W \cdot 2\,H_2O$	60	19.8			60	120	840

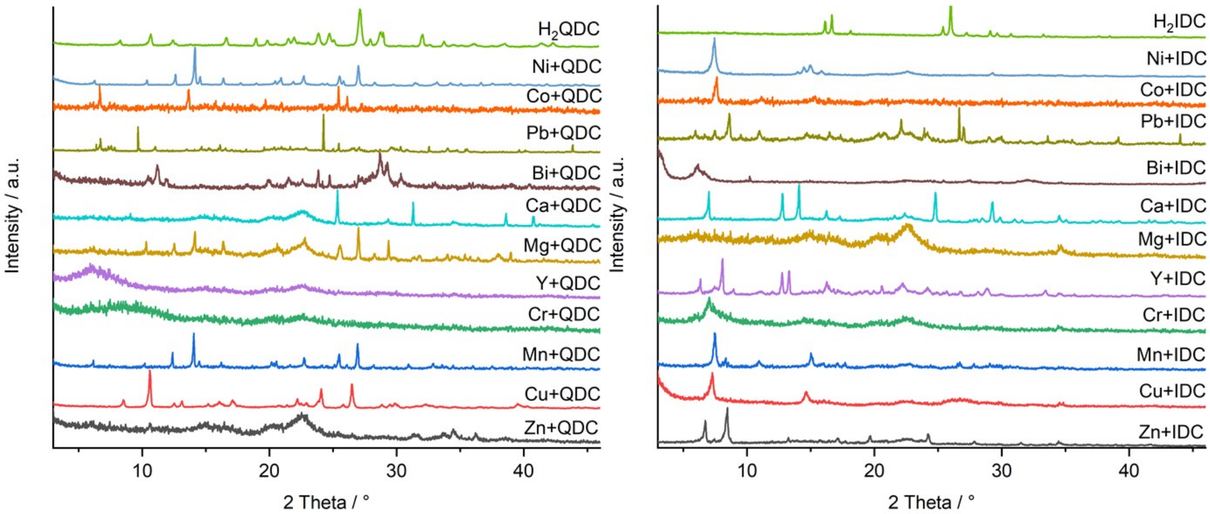

Figure S3: PXRD patterns of the products of the HT-screening with the linker molecules 2,4-quinoline dicarboxylic acid (left) and 2,5-indole dicarboxylic acid (right) with 12 different metal salts compared to the XRD pattern of the respective protonated linker molecule. For the syntheses with Na_2O_4W no PXRD pattern is shown since no solid product could be obtained.

Sorption

To prove that the compound with the highest temperature increase in the optical calorimetry screening is also the compound with the highest CO_2 adsorption capacity, volumetric CO_2 sorption isotherms of the five best performing reaction products were collected (Figure S4).

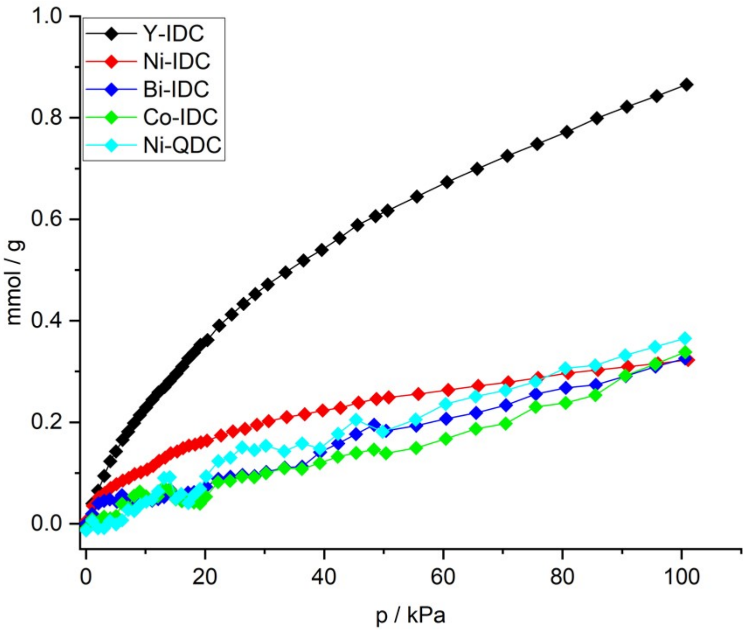

Figure S4: Comparison of the volumetric CO_2 sorption isotherms of the samples with the strongest temperature increase after exposure to CO_2 in the optical calorimetry screening. The poor data quality for the samples besides Y-IDC is due to the small amount of sample available from the screening experiments (ca. 5 mg per sample) and their low CO_2 uptake.

To show, that **CAU-73** can reversibly adsorb water, four consecutive H_2O adsorption cycles were measured at 298 K with an adsorption step at 90 % RH followed by activation at 200 °C.

Sorption experiments were carried out to investigate the adsorption of N_2 in **CAU-73** at 298 K but no significant uptake could be detected (Figure S6**).**

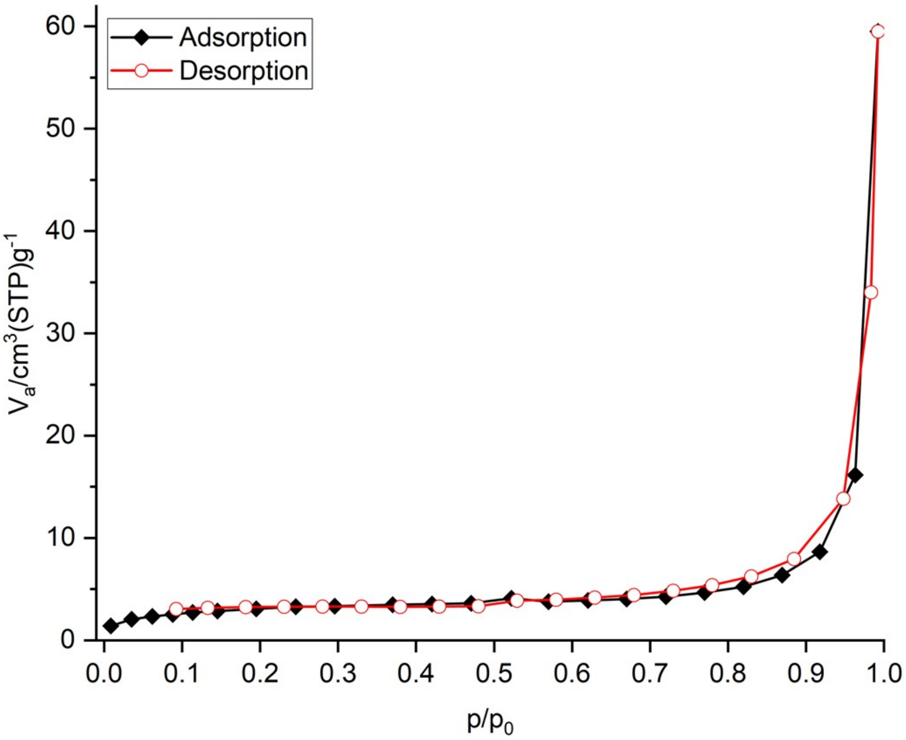

Figure S5: Nitrogen sorption isotherms of **CAU-73** at 77 K.

To ensure, that the material retains its crystallinity after the sorption experiments, powder diffractograms of the samples were collected and compared to the pristine MOFs (Figure S7).

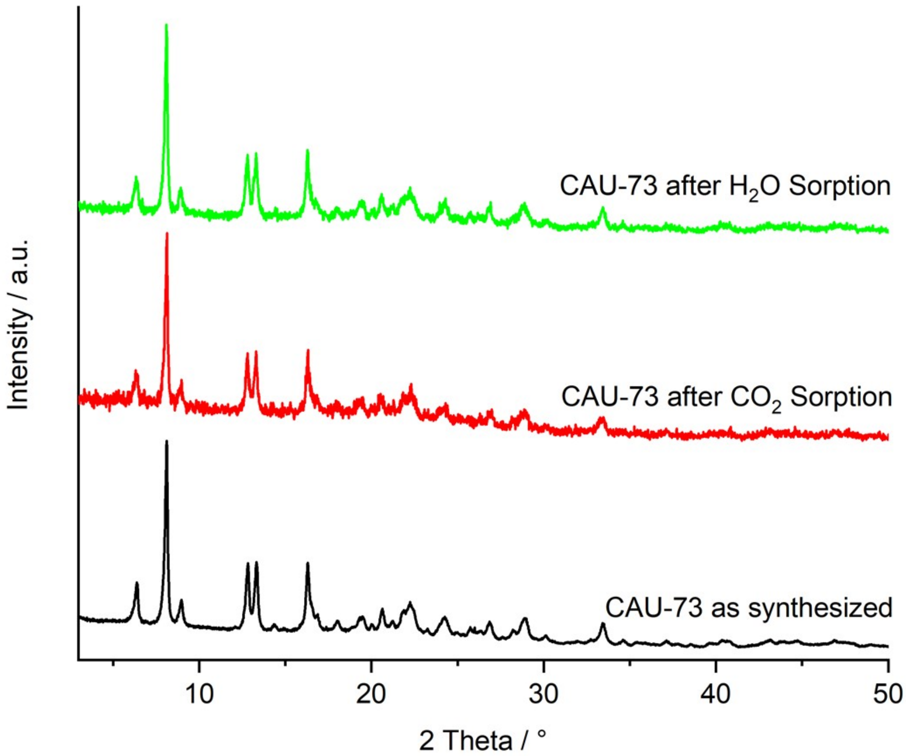

Figure S6: Comparison of the PXRD pattern of **CAU-73** before and after the sorption experiments.

Structure determination

The crystallographic tables for the **CAU-73** compounds with different water contents are summarized in table S3.

Table S3: Crystallographic tables for the three **CAU-73** compounds.

Compound	CAU-73_2.5 H_2O $[Y_2(IDC)_3(H_2O)_2] \cdot 0.5\ H_2O$	CAU-73_1 H_2O $[Y_2(IDC)_3(H_2O)]$	CAU-73_0 H_2O $[Y_2(IDC)_3]$
Method	cRED	cRED	cRED
Chemical Formula	$Y_2C_{30}H_{15}N_3O_{14.5}$	$Y_2C_{30}H_{17}N_3O_{13}$	$Y_2C_{30}N_3O_{12}$
Formula Weight (g/mol)	827.27	803.27	772.15
Calculated Density (g/cm^3)	1.853	1.677	1.679
Z	2	2	2
Resolution (Å)	0.84	0.80	0.87
No. of datasets merged	4	7	11
Rotation range / dataset (degree)	110	100	50
Wavelength / Å	0.02508	0.02508	0.02508
Temperature / K	100(3)	298(3)	523(3)
Completeness (Full 1.7°)	98.6%	99.2%	87.3%
R_{int}	0.3060	0.2048	0.2247
Space group	$P\bar{1}$ (No. 2)	$P\bar{1}$ (No. 2)	$P\bar{1}$ (No. 2)
a / Å	9.58(3)	9.683(12)	9.39(3)
b / Å	11.83(5)	11.981(13)	11.74(5)
c / Å	14.329(8)	15.274(17)	15.51(2)
α / °	100.00(11)	102.56(5)	106.20(14)
β / °	99.1(3)	96.50(6)	99.55(15)
γ / °	107.99(13)	110.022(17)	105.45(7)
V / Å^3	1483(8)	1591(3)	1528(8)
No. unique reflection (F > 4σ(F)/all)	3102/5154	4334/6376	2282/4245
No. of parameters	447	317	425
No. of restraints	471	381	562
$R_1(F > 4\sigma(F))/ R_1(\text{all})$	0.2207/0.2701	0.2141/0.2443	0.2245/0.2818
GooF	1.107	1.071	1.041

PXRD data under ambient conditions was collected and compared to the calculated XRD-patterns for the different **CAU-73** structures to determine the phase that is formed after the synthesis, which is the fully hydrated one with the sum formula $[Y_2(IDC)_3(H_2O)_2] \cdot 0.5\ H_2O$ (Figure S5).

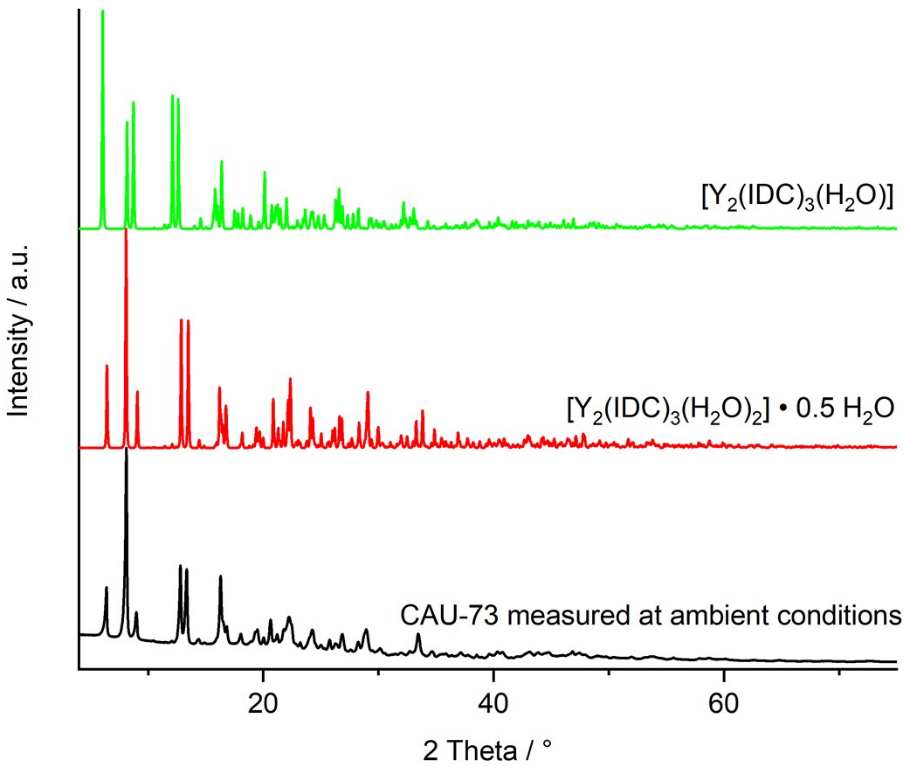

Figure S7: Comparison of the PXRD pattern of **CAU-73** measured at ambient conditions (black) compared to the calculated powder patterns for $[Y_2(IDC)_3(H_2O)_2] \cdot 0.5\ H_2O$ (red) and $Y_2(IDC)_3(H_2O)]$ (green).

Structure description

The CAU-73 compounds crystallize in the triclinic space group $P\bar{1}$ and contain differing amounts of crystallographic water molecules depending on the pressure and temperature they are stored in. At cryogenic conditions, CAU-73 has the composition of $[Y_2(IDC)_3(H_2O)_2] \cdot 0.5\ H_2O$. The inorganic building unit is made up of two crystallographically independent $[YO_7]$ polyhedra each forming a distorted pentagonal bipyramid, which are connected into a chain along the crystallographic *a*-axis via the carboxylate groups of the linker molecules (Figure S9). The coordination environments of both Y ions consist of 6 oxygen atoms from the linker molecules and one additional coordinating water molecule respectively. Each chain is connected to 4 other chains through 6 linker molecules to form a 3D framework with two potential pore channels. One of these channels adopts an open form (marked in green in figure S9) and contains 0.5 adsorbed H_2O molecules per formula unit while the other one (marked in yellow) is held close by hydrogen bonding interactions between two coordinating water molecules (Figure S9). Under reduced pressure or at elevated temperatures, the physisorbed water molecules and the coordinating water molecule that is pointing into the open pore are removed, leading to $[Y_2(IDC)_3(H2O)]$ (Figure S10). This changes the coordination geometry of one of the yttrium ions from pentagonal bipyramidal to octahedral and causes the pore to open up even wider, which is reflected in the elongation of the crystallographic c axis (Table S3). At 250 °C, all water molecules are removed from the compound, leading to fully activated CAU-73 with the composition $[Y_2(IDC)_3]$ and two octahedrally surrounded Y ions (Figure S11).

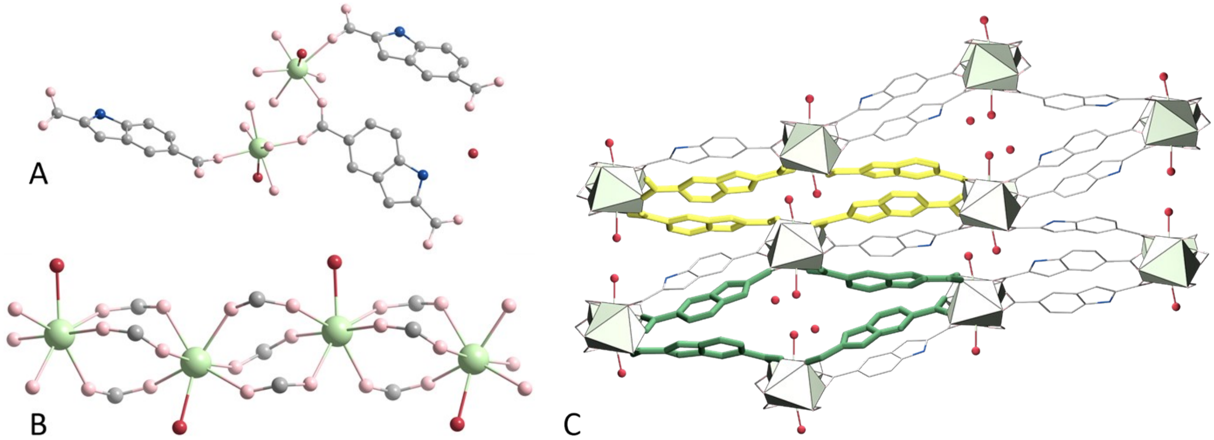

Figure S8: Details of the crystal structure of CAU-73-2.5 H_2O. **A** shows the asymmetric unit, **B** the chain like hybrid IBU running along [100] and **C** the framework with the two different pore channels along [100] depicted in green and yellow. Carbon atoms are shown in grey, nitrogen in blue, yttrium in green, carboxylic oxygen atoms in pink and oxygen atoms belonging to water molecules in red.

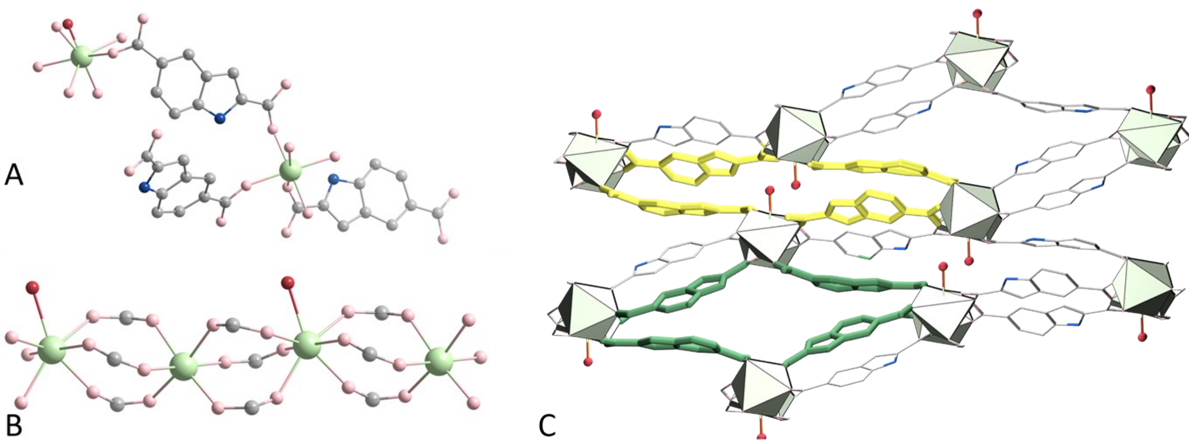

Figure S9: Details of the crystal structure of CAU-73-1 H_2O. **A** shows the asymmetric unit, **B** the chain like hybrid IBU running along [100] and **C** the framework with the two different pore channels along [100] depicted in green and yellow. Carbon atoms are shown in grey, nitrogen in blue, yttrium in green, carboxylic oxygen atoms in pink and oxygen atoms belonging to water molecules in red.

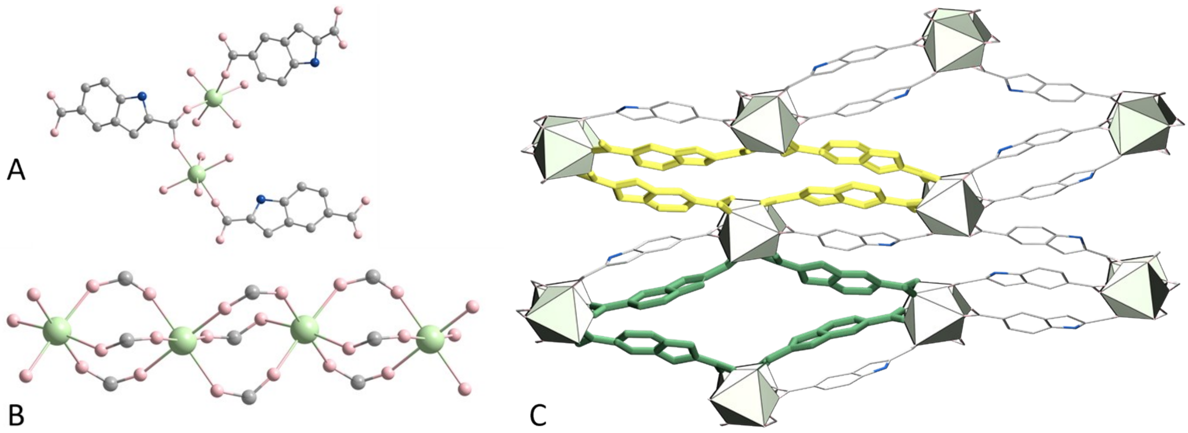

Figure S10: Details of the crystal structure of CAU-73. **A** shows the asymmetric unit, **B** the chain like hybrid IBU running along [100] and **C** the framework with the two different pore channels along [100] depicted in green and yellow. Carbon atoms are shown in grey, nitrogen in blue, yttrium in green and carboxylic oxygen atoms in pink.

IR Spectroscopy

IR spectra of the MOF and the 2,5-indole dicarboxylic acid were collected to gain information about the composition of the compounds and especially about any water molecules that are present in the materials. All bands that were assigned to specific vibrations are marked with asterisks.

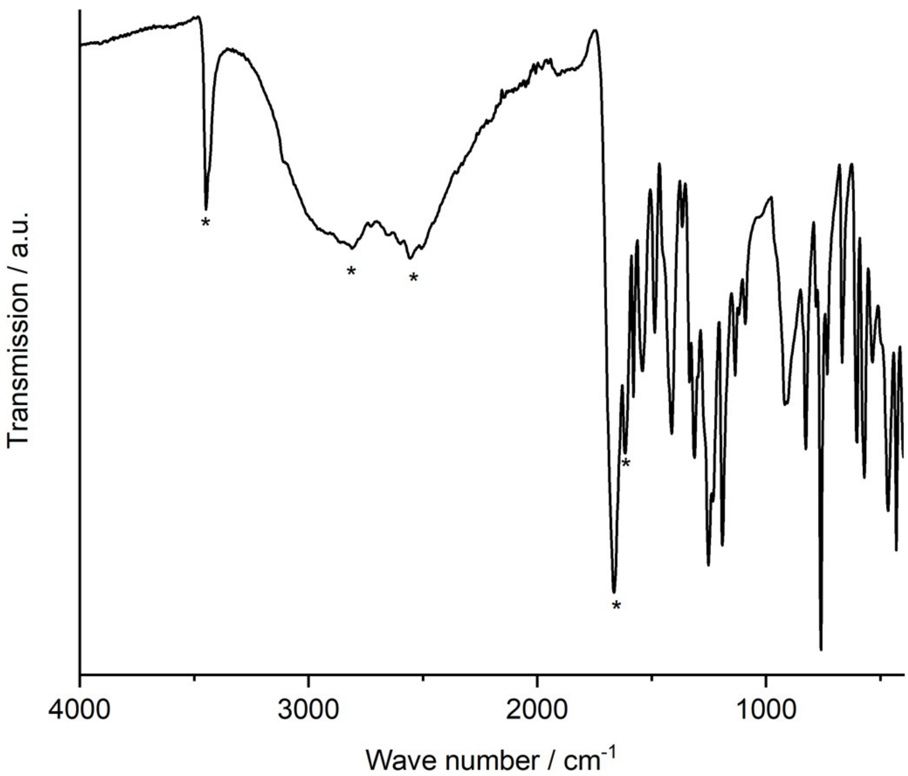

Figure S11: IR spectrum of 2,5-Indole dicarboxylic acid.

Table S4: Assignment of selected vibrations in the IR spectrum of 2,5-indole dicarboxylic acid.

Wave number / cm^{-1}	Vibration
3448	ν(N-H)
2822	ν(O-H) COOH and overtones and combination vibrations
2550	ν(O-H) COOH and overtones and combination vibrations
1666	ν_{as}(C=O)
1616	Indole ring vibration

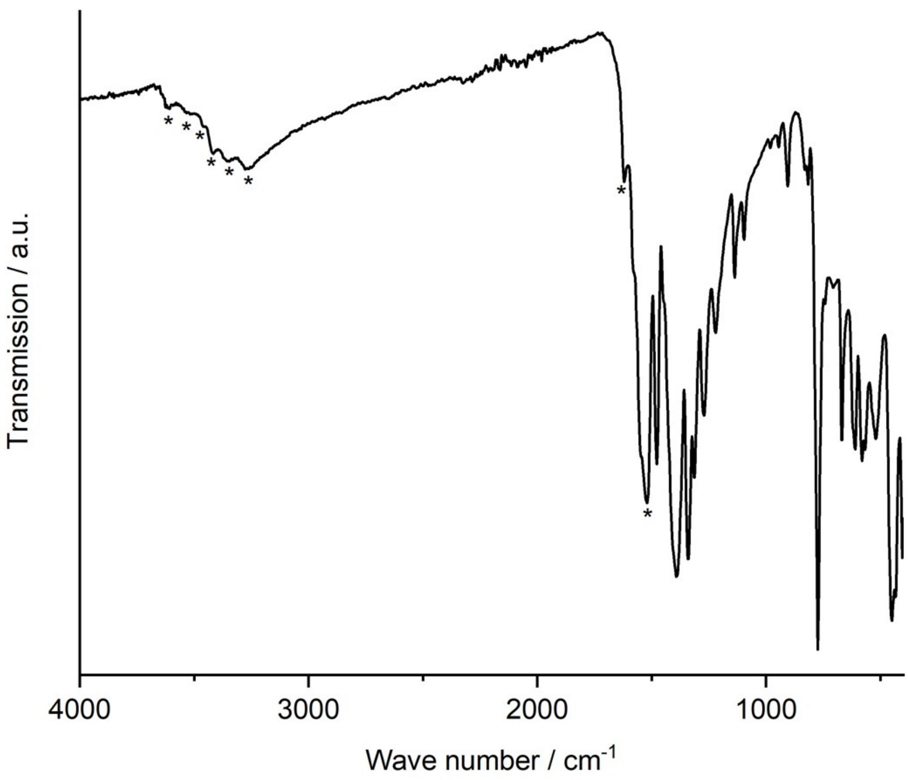

Figure S12: IR spectrum of **CAU-73**.

Table S5 Assignment of selected vibrations in the IR spectrum of **CAU-73.**

Wave number / cm^{-1}	Vibration
3614	ν(O-H)
3510	ν(O-H)
3459	ν(N-H)
3416	ν(N-H)
3349	ν(O-H)
3276	ν(O-H)
1621	Indole ring vibration
1525	ν_{as}(C=O)

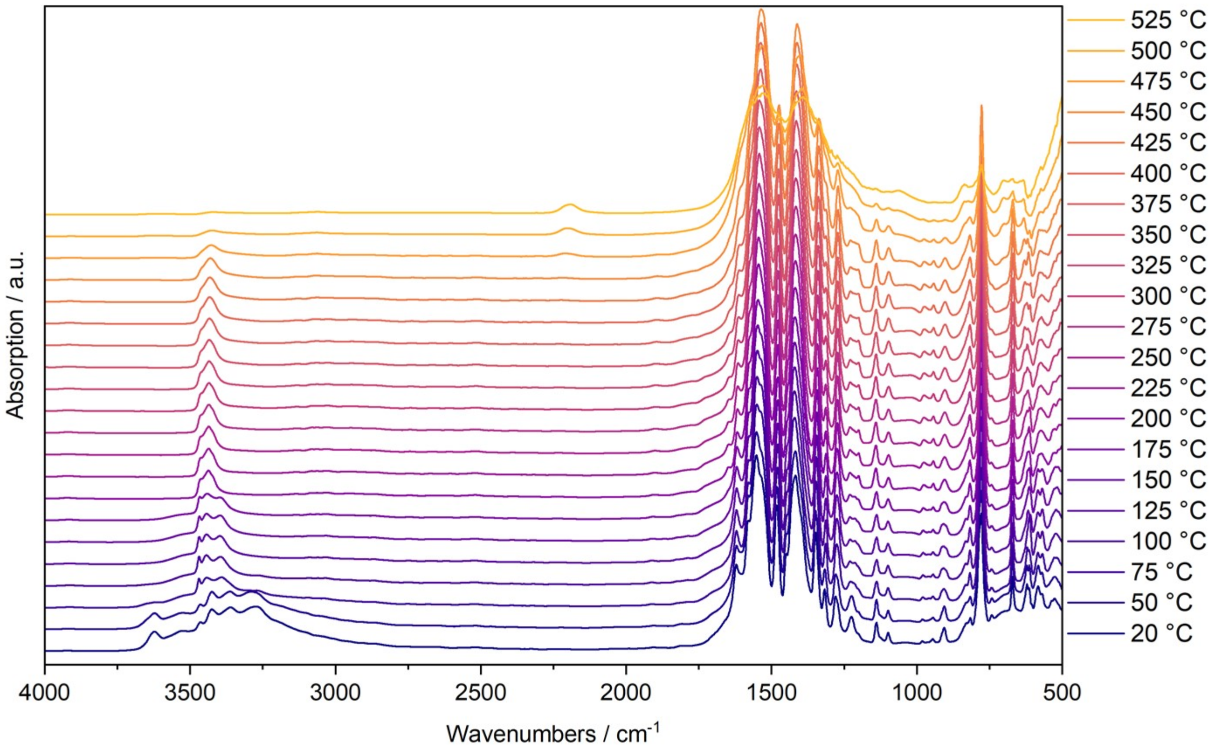

Figure S13: DRIFT spectra of CAU-73 from 20 °C to 525 °C.

Scanning electron microscopy

SEM micrographs of **CAU-73** was collected to obtain information about the particle sizes and morphology.

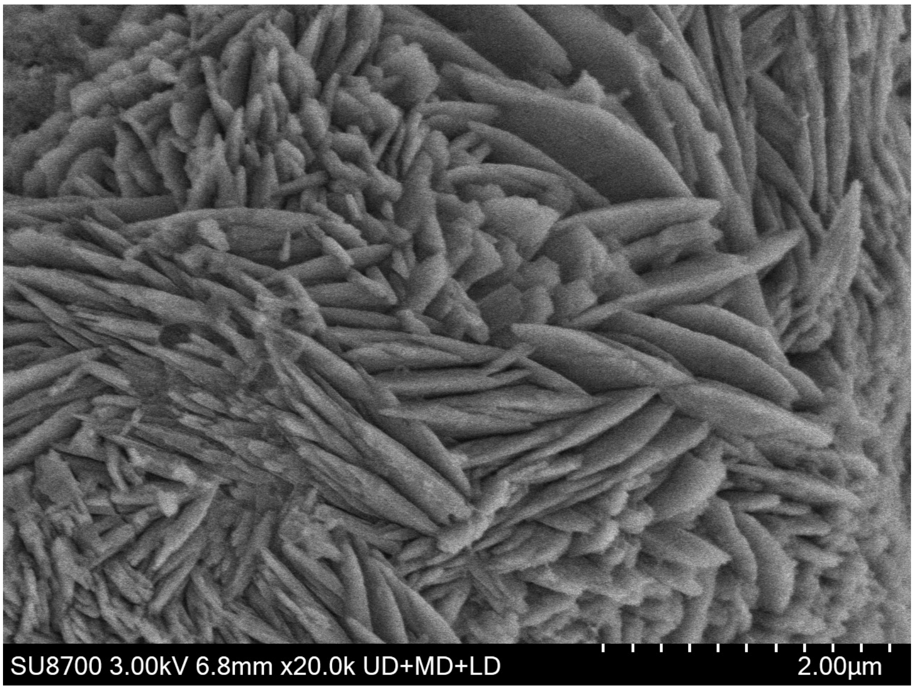

Figure S14: SEM micrograph of **CAU-73** at a magnification of 20k.

Both materials show highly agglomerated crystallites of irregular shapes and polydisperse particle size distributions.

References

(1) Cichocka, M. O.; Ångström, J.; Wang, B.; Zou, X.; Smeets, S. High-throughput continuous rotation electron diffraction data acquisition via software automation. *J. Appl. Cryst.* **2018**, *51*, 1652–1661.

(2) Smeets, S.; Wang, B.; Cichocka, M.O.; Ångström, J.; Wan, W.. *Instamatic*; Zenodo, 2018.

(3) Wang, L.; Chen, Y.; Scaletti Hutchinson, E.; Stenmark, P.; Hofer, G.; Xu, H.; Zou, X. *AutoLEI: An XDS-based Graphical User Interface for Automated Real-time and Offline Batch 3D ED/MicroED Data Processing*; Zenodo, 2025.

(4) Kabsch, W. XDS. *Acta Crystallogr. D Biol. Crystallogr.* **2010**, *66*, 125–132.

(5) Sheldrick, G. M. SHELXT - integrated space-group and crystal-structure determination. *Acta Crystallogr. A Found. Adv.* **2015**, *71*, 3–8.

(6) Sheldrick, G. M. Crystal structure refinement with SHELXL. *Acta Crystallogr. C Struct. Chem.* **2015**, *71*, 3–8.

(7) Dolomanov, O. V.; Bourhis, L. J.; Gildea, R. J.; Howard, J. A. K.; Puschmann, H. OLEX2 : a complete structure solution, refinement and analysis program. *J. Appl. Cryst.* **2009**, *42*, 339–341.

(8) Altomare, A.; Cuocci, C.; Giacovazzo, C.; Moliterni, A.; Rizzi, R.; Corriero, N.; Falcicchio, A. *EXPO2013*: A kit of tools for phasing crystal structures from powder data. *J. Appl. Cryst.* **2013**, *46*, 1231–1235.

(9) Coelho, A. A. TOPAS and TOPAS-Academic : an optimization program integrating computer algebra and crystallographic objects written in C++. *J. Appl. Cryst.* **2018**, *51*, 210–218.